

Multiscale modeling of fiber reinforced materials via non-matching immersed methods

Giovanni Alzetta^a, Luca Heltai^a

^a*SISSA-International School for Advanced Studies
via Bonomea 265, 34136 Trieste - Italy*

Abstract

Fiber reinforced materials (FRMs) can be modeled as bi-phasic materials, where different constitutive behaviors are associated with different phases. The numerical study of FRMs through a full geometrical resolution of the two phases is often computationally infeasible, and therefore most works on the subject resort to homogenization theory, and exploit strong regularity assumptions on the fibers distribution. Both approaches fall short in intermediate regimes where lack of regularity does not justify a homogenized approach, and when the fiber geometry or their numerosity render the fully resolved problem numerically intractable.

In this paper, we propose a distributed Lagrange multiplier approach, where the effect of the fibers is superimposed on a background isotropic material through an independent description of the fibers. The two phases are coupled through a constraint condition, opening the way for intricate fiber-bulk couplings as well as allowing complex geometries with no alignment requirements between the discretisation of the background elastic matrix and the fibers.

We analyze both a full order coupling, where the elastic matrix is coupled with fibers that have a finite thickness, as well as a reduced order model, where the position of their centerline uniquely determines the fibers. Well posedness, existence, and uniqueness of solutions are shown both for the continuous models, and for the finite element discretizations. We validate our approach against the models derived by the rule of mixtures, and by the Halpin-Tsai formulation.

Keywords: Immersed boundary method, finite element method, fiber composites, Lagrange multipliers

1. Introduction

Numerous engineering applications require the efficient solution of partial differential equations involving multiple, complex geometries on different phases; *composite materials* are the prototypical example of such problems. During the past fifty years, the interest

Email addresses: giovannialzetta@gmail.com (Giovanni Alzetta), luca.heltai@sissa.it (Luca Heltai)

in composite materials flourished multiple times; it began for their applications to new materials in multiple fields, such as aerospace engineering [26], civil engineering [47], and materials science [9, 45].

During the nineties, the increasing importance of biomechanics in life sciences led to the development of numerous models describing, e.g., arterial walls [34], soft tissues [32], and muscle fibers [35].

Recent years saw the rise of new application fields, such as the study of natural fiber composites [53], and engineering methods to accurately recover the three-dimensional structure of a material sample, e.g., [36, 37].

From the first studies on composites, it has been clear that their properties are strongly dependent on their internal structure: the volume ratio between each component, the orientation, the shape, all contribute substantially to the material's properties [26, 27]. One of the most wide-spread and significant example of composites is that of Fiber Reinforced Materials (FRMs), where thin, elongated structures (the fibers) are immersed in an underlying isotropic material (the elastic matrix).

We may separate the approaches used to study FRMs into two broad groups: i) “*homogenization methods*”, which study a complex inhomogeneous body by approximating it with a fictitious homogeneous body that behaves globally in the same way [61], and ii) “*fully resolved*” methods, which use separate geometrical and constitutive descriptions for the elastic matrix and the individual fibers.

As examples of analytical “*homogenization methods*” we recall the rule of mixtures [25] and the *empirical* Halpin-Tsai equations [24], used to study a transversely isotropic unidirectional composite, where fibers are uniformly distributed and share the same orientation. The development of homogenization theory led, in recent years, to more complex models, e.g., [33, 8].

More intricate homogenization approaches rely on numerical methods to provide a “cell” behaviour, which is then replicated using periodicity, using, e.g., the Finite Element Method [1, 50, 42], Fourier transforms [48, 49, 21], or Stochastic Methods [43].

The fundamental limit of all “*homogenization methods*” approaches is the impossibility of adapting them to study composites with little regularity. In these cases, the different phases are typically modeled separately, as a continuum. This approach began with Pipkin [54] on two dimensional membranes, and was then expanded to three dimensional examples by others (see, e.g., [39] for a detailed bibliography).

Fully resolved methods allow richer structures, but require a high numerical resolution, especially when material phases have different scales. The complex meshing and coupling often result in an unbearable computational cost, limiting the use of these methods.

The purpose of this paper is to introduce an approach which is fit for materials that have *intermediate* properties, i.e., they possess no particular regularity, and are made by a relatively high number of fiber components. Similarly to [55], our model is inspired by the Immersed Boundary Method (IBM) [52], and by its variational counterparts [13, 28, 30, 57, 31], where the elastic matrix and the fibers are modeled independently, and coupled through a non-slip condition. The model we present can be interpreted as a variation of the embedded reinforced method (see [22] and the references therein), where we aim at providing an efficient numerical method for FRMs that allows the modeling of complex networks of fibers, where one may also be interested in the elastic properties of single fibers, without requiring the resolution of the single fibers in the background

elastic matrix. From the computational point of view, this approach allows the use of two independent discretizations: one describing the fibers, and one describing the *whole domain*, i.e., both the elastic matrix and the fibers. A distributed Lagrange multiplier is used to couple the independent grids, following the same spirit of the finite element immersed boundary method [11, 13], separating the Cauchy stress of the whole material into a background uniform behavior and into an *excess* elastic behavior on the fibers.

Section 2 introduces the classical fully resolved model of a collection of fibers immersed in an elastic matrix. For simplicity, we do not include dissipative terms, and restrict our study to linearly elastic materials. The problem is then reformulated exploiting classical results of mixed methods (see Chapter 4 of [10]), following ideas similar to those found in [12], proving that both the continuous and discrete formulations we propose are well-posed with a unique solution.

The use of a full three dimensional model for the fibers still results in high computational costs; the obvious simplification would be to approximate the fibers with one-dimensional structures. This approach is non-trivial because the theoretical solution of the fully resolved variational problem does not possess enough Sobolev regularity to allow the restriction of a three-dimensional field to a one-dimensional domain. A possible workaround involves the use of weighted Sobolev spaces, combined with graded meshes [19, 18]. This approach remains unfeasible when the number of fibers is large. In Section 3, we propose and analyze an alternative strategy, where under some additional assumptions we construct a $3D-1D$ coupling that relies on local averaging techniques. A similar procedure is used in [29] to model vascularized tissues. To conclude, we validate our thin fiber model in Section 4, and draw some conclusions in Section 5.

2. Three-dimensional model

Many bi-phasic materials present a relatively simple fiber structure but result in a very intricate elastic matrix. Consider, for example, Figure 1: constructing a discretization grid for the fibers themselves maybe simple enough, but building a fully resolved grid for the *surrounding* elastic matrix, in this case, may require excessive resolution, and result in a computationally hard problem to solve. We wish to describe a new approach, where we substitute the complex mesh needed for the elastic matrix with a simple one describing the whole domain, and overlap the fiber structure independently with respect to the background grid, and couple the two systems via distributed Lagrange multipliers.

2.1. Problem formulation

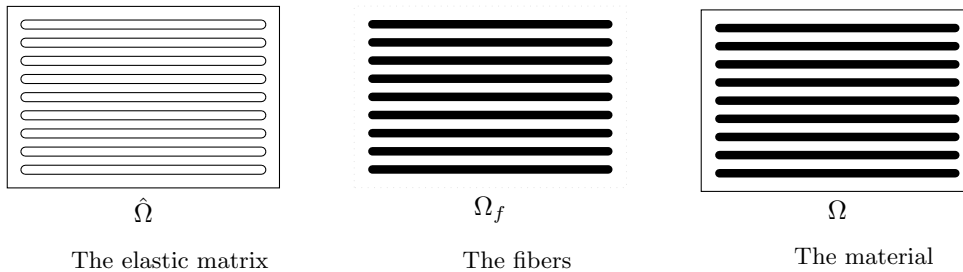
As a model bi-phasic material, we consider a linearly elastic fiber reinforced material, in the quasi-static small strain regime. We consider continuous fibers with a perfect bond between the two phases (see [16, Chapter 16]), leading to a no-slip condition between the fibers and the elastic matrix. The extension to finite strain elasticity, dynamic problems, or non-perfect bonds do not present additional difficulties and will be the subject of future investigations.

To describe the composite, we use a connected, bounded, Lipschitz domain $\Omega \subset \mathbb{R}^d$ of dimension $d = 3$, composed of a fiber phase $\Omega_f \subset \Omega$, and an elastic matrix $\hat{\Omega} := \Omega \setminus \Omega_f \subset \mathbb{R}^d$, which we assume to be a connected, Lipschitz domain. We describe each



Figure 1: An example of a fiber structure for which the mesh generation for the fibers would be trivial, but the resulting three-dimensional elastic matrix would be much more expensive to resolve in full.

of the $n_f \in \mathbb{N}$ fibers with a connected, Lipschitz domain and Ω_f is obtained as the union of these (possibly overlapping) domains.



Example of a two-dimensional section of an FRM with uniformly oriented fibers.

Remark. *The results of this section hold for a general domain Ω_f , union of multiple components with the required regularity. The property of the fibers of being thin, elongated, structures, is only needed for the model of Section 3, and plays no role in this section.*

Given a continuous displacement field $u: \Omega \rightarrow \mathbb{R}^d$, representing a deformation from the equilibrium configuration, the corresponding stress tensor on Ω can be expressed using the stress-strain law [23]:

$$S[u] = \mathbb{C}\nabla u,$$

where \mathbb{C} is a symmetric 4th order tensor that takes the form:

$$\mathbb{C} = \begin{cases} \mathbb{C}_\Omega & \text{in } \hat{\Omega}, \\ \mathbb{C}_f & \text{in } \Omega_f. \end{cases} \quad (1)$$

Here \mathbb{C}_Ω and \mathbb{C}_f are assumed to be constant over their respective domains, and represent the elasticity tensors of the elastic matrix and of the fibers. The assumption of perfect bonds between the fibers and the elastic matrix (see [16, Chapter 16]) allows one to define the full order problem as a single elasticity problem on the union of the two domains, with pecewise elastic properties. This assumption may be relaxed by reformulating the fiber elasticity equations and the elastic matrix elasticity equations separately, and coupling them with appropriate interface (or bonding) conditions.

The classical formulation of static linear elasticity can be thought of as a force balance equation (see, for example, [23]):

Problem 1 (Classic Strong Formulation). *Given an external force density field b , find the displacement u such that*

$$\begin{aligned} -\operatorname{div}(\mathbb{C}u) &= b && \text{in } \Omega, \\ u &= 0 && \text{on } \partial\Omega. \end{aligned} \quad (2)$$

Due to the piecewise nature of \mathbb{C} , it is natural to reformulate Problem 1 into a variational or weak formulation. Given a subset D of $\partial\Omega$, we introduce the notation for the subspace of the Sobolev space $H^1(\Omega)$ with functions vanishing on a subset D of the boundary $\partial\Omega$:

$$H_{0,D}^1(\Omega)^d := \{v \in H^1(\Omega)^d : v|_D = 0\},$$

with norm $\|\cdot\|_V = \|\cdot\|_{H^1(\Omega)} := \|\cdot\|_\Omega + \|\nabla \cdot\|_\Omega$, where the symbol $\|\cdot\|_A$ represents the $L^2(A)$ norm over the measurable set $A \subset \Omega$, and $(\cdot, \cdot)_A$ represents the L^2 scalar product on the given domain A . We define the following space:

$$V := (H_{0,\partial\Omega}^1(\Omega))^d = \{v \in H^1(\Omega)^d : v|_{\partial\Omega} = 0\},$$

The standard weak formulation reads:

Problem 2 (Classic Weak Formulation). *Given $b \in L^2(\Omega)^d$, find $u \in V$ such that:*

$$(\mathbb{C}\nabla u, \nabla v)_\Omega = (b, v)_\Omega \quad \forall v \in V. \quad (3)$$

The main idea behind our reformulation is to rewrite Problem 2 into an equivalent form, where we define two independent functional spaces. The novelty we introduce is to define the functional spaces on Ω and Ω_f , and not on $\hat{\Omega}$ and Ω_f . To achieved this, we define two fictitious materials: one with the same properties of the elastic matrix, occupying the full space Ω , and one describing the “excess elasticity” of the fibers separately, defined on Ω_f only. The first step in this direction is to split the left-hand side of Equation (3) on the two domains:

$$\begin{aligned} (\mathbb{C}\nabla u, \nabla v)_\Omega &= (\mathbb{C}_f \nabla u, \nabla v)_{\Omega_f} + (\mathbb{C}_\Omega \nabla u, \nabla v)_{\hat{\Omega}} \\ &= (\mathbb{C}_f \nabla u, \nabla v)_{\Omega_f} + \underbrace{(\mathbb{C}_\Omega \nabla u, \nabla v)_{\hat{\Omega}} + (\mathbb{C}_\Omega \nabla u, \nabla v)_{\Omega_f}}_{\Omega} - (\mathbb{C}_\Omega \nabla u, \nabla v)_{\Omega_f} \\ &= (\mathbb{C}_\Omega \nabla u, \nabla v)_\Omega + (\delta \mathbb{C}_f \nabla u, \nabla v)_{\Omega_f}, \end{aligned}$$

where $\delta\mathbb{C}_f := \mathbb{C}_f - (\mathbb{C}_\Omega)|_{\Omega_f}$.

For simplicity, we improperly use the expression “elastic matrix equation” and “fiber equation”, even though they should be really considered as the “whole domain equation”, and a “delta fiber equation”. This formal separation does not change the original variational problem, which can still be stated explicitly: given $b \in L^2(\Omega)^d$, find $u \in V$ such that:

$$(\mathbb{C}_\Omega \nabla u, \nabla v)_\Omega + (\delta\mathbb{C}_f \nabla u, \nabla v)_{\Omega_f} = (b, v)_\Omega \quad \forall v \in V. \quad (4)$$

The boundary of the domain Ω induces a natural splitting on the boundary of the fibers: we define the following partition of $\partial\Omega_f$:

$$B_i := \partial\Omega_f \setminus \partial\Omega \quad (5)$$

$$B_e := \partial\Omega \cap \partial\Omega_f, \quad (6)$$

where B_i is the interface between the fibers and the elastic matrix, while B_e is the interface between the fibers the exterior part of Ω , that lies on the boundary $\partial\Omega$. Next we define the restriction of $H_0^1(\Omega)^d$ on the fibers:

$$W := (H_{0,B_e}^1(\Omega_f))^d, \quad (7)$$

and separate the solution of Problem 2 in two components, one describing the whole material, the other describing only the fibers.

When reformulating the problem with two independent variables, the perfect bond condition between the fibers and the elastic matrix must be imposed via a volumetric non-slip constraint on the solution $(u, w) \in V \times W$:

$$u|_{\Omega_f} = w. \quad (8)$$

The described setting is similar to the distributed Lagrange multiplier method used to model fluid structure interaction problems with non-matching discretisations, as described in [11, 5, 14].

The result is a constrained minimization problem:

$$u, w = \arg \inf_{\substack{(u,v) \in V \times W \\ u|_{\Omega_f} = w}} \psi(u, w), \quad (9)$$

where we defined the total elastic energy of the system as

$$\psi(u, w) = \frac{1}{2}(\mathbb{C}_\Omega \nabla u, \nabla u)_\Omega + \frac{1}{2}(\delta\mathbb{C}_f \nabla w, \nabla w)_{\Omega_f} - (b, u)_\Omega. \quad (10)$$

To impose the non-slip constraint of Equation (8), we use the duality product $W' \times W$ as in [12]. We define $Q := W'$, and enforce the perfect bond on the fibers by asking that

$$\langle q, u|_{\Omega_f} - w \rangle_{Q \times W} = 0 \quad \forall q \in Q. \quad (11)$$

For simplicity we will omit the subscript $Q \times W$ from now on.

The constrained minimization expressed in Equation (9) is equivalent to the saddle point problem:

$$u, w, \lambda = \arg \inf_{\substack{u \in V \\ w \in W}} \left(\arg \sup_{\lambda \in Q} \psi(u, w, \lambda) \right), \quad (12)$$

where the constraint is imposed weakly as in 11 through a Lagrange multiplier:

$$\psi(u, w, \lambda) := \frac{1}{2}(\mathbb{C}_\Omega \nabla u, \nabla u)_\Omega + \frac{1}{2}(\delta \mathbb{C}_f \nabla w, \nabla w)_{\Omega_f} + \langle \lambda, u|_{\Omega_f} - w \rangle - (b, u)_\Omega.$$

A solution to Equation (12) is obtained by solving the Euler-Lagrange equation:

$$\langle D_u \psi, v \rangle + \langle D_w \psi, y \rangle + \langle D_\lambda \psi, q \rangle = 0 \quad \forall v \in V, \forall y \in W, \forall q \in Q, \quad (13)$$

that is:

Problem 3 (Saddle Point Weak Formulation). *Given $b \in L^2(\Omega)^d$, find $u \in V, w \in W, \lambda \in Q$ such that:*

$$(\mathbb{C}_\Omega \nabla u, \nabla v)_\Omega + \langle \lambda, v|_{\Omega_f} \rangle = (b, v)_\Omega \quad \forall v \in V \quad (14)$$

$$(\delta \mathbb{C}_f \nabla w, \nabla y)_{\Omega_f} - \langle \lambda, y \rangle = 0 \quad \forall y \in W \quad (15)$$

$$\langle q, u|_{\Omega_f} - w \rangle = 0 \quad \forall q \in Q, \quad (16)$$

or, equivalently,

$$\begin{array}{rclcl} \mathcal{K}_\Omega u & + \mathcal{B}^T \lambda & = (b, \cdot)_\Omega & \text{in } V' \\ & \mathcal{K}_f w & - \mathcal{M}^T \lambda & = 0 & \text{in } W' \\ \mathcal{B} u & - \mathcal{M} w & & = 0 & \text{in } Q', \end{array} \quad (17)$$

where

$$\begin{array}{ll} \mathcal{K}_\Omega: V \rightarrow V' & \langle \mathcal{K}_\Omega u, \cdot \rangle := (\mathbb{C}_\Omega \nabla u, \nabla \cdot)_\Omega \\ \mathcal{K}_f: W \rightarrow W' & \langle \mathcal{K}_f w, \cdot \rangle := (\delta \mathbb{C}_f \nabla w, \nabla \cdot)_{\Omega_f} \\ \mathcal{B}: V \rightarrow Q' & \langle \mathcal{B} u, \cdot \rangle := \langle \cdot, u|_{\Omega_f} \rangle \\ \mathcal{M}: W \rightarrow Q' & \langle \mathcal{M} w, \cdot \rangle := \langle \cdot, w \rangle. \end{array} \quad (18)$$

2.2. Well-posedness, existence and uniqueness

Existence and uniqueness follow from standard saddle point theory [10]. We introduce the product Hilbert space, with its norm:

$$\begin{aligned} \mathbb{V} &:= V \times W, \\ \|(u, w)\|_{\mathbb{V}}^2 &:= \|u\|_V^2 + \|w\|_W^2, \end{aligned}$$

and we indicate with $\mathbf{u} := (u, w), \mathbf{v} := (v, y)$ the elements of \mathbb{V} . We define the bilinear forms

$$\begin{aligned} \mathbb{F}: \mathbb{V} \times \mathbb{V} &\longrightarrow \mathbb{R} \\ (\mathbf{u}, \mathbf{v}) &\longmapsto \langle \mathcal{K}_\Omega u, v \rangle + \langle \mathcal{K}_f w, y \rangle = (\mathbb{C}_\Omega \nabla u, \nabla v)_\Omega + (\delta \mathbb{C}_f \nabla w, \nabla y)_{\Omega_f}, \\ \mathbb{E}: \mathbb{V} \times Q &\longrightarrow \mathbb{R} \\ (\mathbf{u}, q) &\longmapsto \langle \mathcal{B} u, q \rangle - \langle \mathcal{M} w, q \rangle = \langle q, v|_{\Omega_f} - w \rangle, \end{aligned}$$

with which we reformulate the problem as: find $\mathbf{u} \in \mathbb{V}, \lambda \in Q$ such that

$$\begin{aligned} \mathbb{F}(\mathbf{u}, \mathbf{v}) + \mathbb{E}(\mathbf{v}, \lambda) &= (b, v)_\Omega & \forall \mathbf{v} := (v, y) \in \mathbb{V}, \\ \mathbb{E}(\mathbf{u}, q) &= 0 & \forall q \in Q. \end{aligned} \quad (19)$$

Proposition 2.1. *There exists a constant $\alpha_1 > 0$ such that:*

$$\inf_{q \in Q} \sup_{(v, w) \in \mathbb{V}} \frac{\langle q, v|_{\Omega_f} - w \rangle}{\|(v, w)\|_{\mathbb{V}} \|q\|_Q} \geq \alpha_1.$$

Moreover $\alpha_1 = 1$.

The proof for this proposition, and its discrete version, are variations on the one found in [12].

Proof. The non slip condition is given by the duality pairing between $Q = W'$ and W ; by definition of the norm in the dual space Q :

$$\begin{aligned} \|q\|_Q &= \sup_{w \in W} \frac{\langle q, w \rangle}{\|w\|_Q} \\ &\leq \sup_{v \in V, w \in W} \frac{\langle q, v|_{\Omega_f} - w \rangle}{(\|w\|_Q^2 + \|v\|_V^2)^{\frac{1}{2}}}, \end{aligned}$$

where the last inequality can be proven fixing $v = 0$. The final statement is found dividing by $\|q\|_Q$ and taking the $\inf_{q \in Q}$. \square

Notice that $\alpha_1 = 1$, and does not depend on the two domains or on the two spaces.

Proposition 2.2. *Assume \mathbb{C}_Ω and \mathbb{C}_f to be strongly elliptic with constants c_Ω and c_f respectively, such that $c_f > c_\Omega > 0$; then there exists a constant $\alpha_2 > 0$ such that:*

$$\inf_{(u, w) \in \ker \mathbb{E}} \sup_{(v, y) \in \ker \mathbb{E}} \frac{(\mathbb{C}_\Omega \nabla u, \nabla v)_\Omega + (\delta \mathbb{C}_f \nabla w, \nabla y)_{\Omega_f}}{\|(v, y)\|_{\mathbb{V}} \|(u, w)\|_{\mathbb{V}}} \geq \alpha_2.$$

Proof. An immediate consequence of the hypotheses is that $\delta \mathbb{C}_f$ is elliptic of constant $c_f - c_\Omega$. Following the proof for a similar statement found in [5, 14], given an element $(v, y) \in \ker(\mathbb{E})$, the fact that $v|_{\Omega_a} = y$ allows to use the Poincaré inequality on v to control the norm of y ; for every $(u, w) \in \ker(\mathbb{E})$:

$$\begin{aligned} &\sup_{(v, y) \in \ker(\mathbb{E})} \frac{(\mathbb{C}_\Omega \nabla u, \nabla v)_\Omega + (\delta \mathbb{C}_f \nabla w, \nabla y)_{\Omega_f}}{\|(v, y)\|_{\mathbb{V}}} \\ &\geq \frac{c_\Omega (\nabla u, \nabla u)_\Omega + (c_f - c_\Omega) (\nabla w, \nabla w)_{\Omega_f}}{\|(u, w)\|_{\mathbb{V}}} \\ &\geq \frac{c_p \min(c_\Omega, c_f - c_\Omega)}{2} \frac{(u, u)_{H^1(\Omega)} + (w, w)_{H^1(\Omega_f)}}{\|(u, w)\|_{\mathbb{V}}} \\ &\geq \alpha_2 \|(u, w)\|_{\mathbb{V}}, \end{aligned}$$

where we used the Poincaré inequality with its positive constant c_p on $u \in V$, with $\alpha_2 := \frac{c_p \min(c_\Omega, c_f - c_\Omega)}{2}$, and we used the scalar product of $H^1(\Omega)^d$:

$$(u, u)_{H^1(\Omega)} := (u, v)_\Omega + (\nabla u, \nabla v)_\Omega,$$

and the analogous one for $H^1(\Omega_f)^d$. The final statement is obtained dividing by $\|(u, w)\|_V$ and considering the $\inf_{(u, w) \in \ker \mathbb{E}}$. \square

Remark. *This paper does not intend to focus on the choice of elastic tensors. Strong ellipticity is a common property among them, and holds in the case of linearly elastic materials (see e.g. [46]): let $u \in V$, $w \in W$*

$$\mathbb{C}_\Omega \nabla u := 2\mu_\Omega E u + \lambda_\Omega (\text{tr} \nabla u) I = 2\mu_\Omega E u + \lambda_\Omega (\text{div} u) I \quad (20)$$

$$\mathbb{C}_f \nabla w := 2\mu_f E w + \lambda_f (\text{tr} \nabla w) I = 2\mu_f E w + \lambda_f (\text{div} w) I \quad (21)$$

$$\begin{aligned} \delta \mathbb{C}_f \nabla w &:= 2(\mu_f - \mu_\Omega) E w + (\lambda_f - \lambda_\Omega) (\text{tr} \nabla w) I \\ &= 2\mu_\delta E w + \lambda_\delta (\text{div} w) I, \end{aligned} \quad (22)$$

where $\mu_\delta := \mu_f - \mu_\Omega$ and $\lambda_\delta := \lambda_f - \lambda_\Omega$, and $E u = \frac{\nabla u + \nabla u^T}{2}$ is the symmetric gradient. These are the elastic tensors we use in Section 4, for our numerical tests.

Propositions 2.2 and 2.1 imply that the inf-sup conditions are satisfied, and that Problem 3 is well-posed, and has a unique solution.

2.3. Finite element discretization

The distributed Lagrange formulation of Problem 3 makes it possible to use independent triangulations for its numerical solution. Consider the family $\mathcal{T}_h(\Omega)$ of regular meshes in Ω , and a family $\mathcal{T}_h(\Omega_f)$ of regular meshes in Ω_f , where we denote by h the maximum diameter of the elements of the two triangulations. We assume that no geometrical error is committed when meshing, i.e., $\Omega = \bigcup_{T_h \in \mathcal{T}_h(\Omega)} T_h$, and $\Omega_f = \bigcup_{S_h \in \mathcal{T}_h(\Omega_f)} S_h$. We consider two independent finite element spaces $V_h \subset V$, and $W_h \subset W$, and we take $Q_h = W_h$. All finite dimensional spaces are endowed with the norms of their continuous counterparts.

Problem 4 (Discrete Weak Formulation). *Given $b \in L^2(\Omega)^d$, find $u_h \in V_h$, $w_h \in W_h$, $\lambda_h \in Q_h$ such that:*

$$(\mathbb{C}_\Omega \nabla u_h, \nabla v_h)_\Omega + \langle \lambda_h, v_h |_{\Omega_f} \rangle = (b, v_h)_\Omega \quad \forall v_h \in V_h, \quad (23)$$

$$(\delta \mathbb{C}_f \nabla w_h, \nabla y_h)_{\Omega_f} - \langle \lambda_h, y_h \rangle = 0 \quad \forall y_h \in W_h, \quad (24)$$

$$\langle q_h, u_h |_{\Omega_f} - w_h \rangle = 0 \quad \forall q_h \in Q_h. \quad (25)$$

Existence, well posedness, and convergence are guaranteed if the classical discrete inf-sup conditions are satisfied:

Proposition 2.3. *Assume that the L^2 projection*

$$P_W : W \rightarrow W_h \subset L^2(\Omega_f)$$

is continuous and H^1 -stable, i.e., there exists a positive constant c_W such that for all $w \in W$:

$$\|\nabla(P_W w)\|_{\Omega_f} \leq c_W \|\nabla w\|_{\Omega_f}. \quad (26)$$

Then there exists a constant $\alpha_3 > 0$, independent of h , such that:

$$\inf_{q_h \in Q_h} \sup_{(v_h, w_h) \in \mathbb{V}_h} \frac{\langle q_h, v_h|_{\Omega_f} - w_h \rangle}{\|(v_h, w_h)\|_{\mathbb{V}} \|q_h\|_Q} \geq \alpha_3.$$

Proof. For every $q_h \in Q_h$, by definition of the Q norm, and by property (26), there exists $\hat{w} \in W$ such that:

$$\|q_h\|_Q = \sup_{w \in W} \frac{\langle q_h, w \rangle}{\|w\|_W} = \frac{\langle q_h, \hat{w} \rangle}{\|\hat{w}\|_W} = \frac{\langle q_h, P_W \hat{w} \rangle}{\|\hat{w}\|_W} \leq c_W \frac{\langle q_h, P_W \hat{w} \rangle}{\|P_W \hat{w}\|_W}. \quad (27)$$

Therefore,

$$\begin{aligned} \|q_h\|_Q &\leq c_W \frac{\langle q_h, P_W \hat{w} \rangle}{\|P_W \hat{w}\|_W} \leq c_W \sup_{w_h \in W_h} \frac{\langle q_h, w_h \rangle}{\|w_h\|_W} \\ &\leq c_W \sup_{v_h \in V_h, w_h \in W_h} \frac{\langle q_h, v_h|_{\Omega_f} - w_h \rangle}{(\|w_h\|_W^2 + \|v_h\|_V^2)^{\frac{1}{2}}}, \end{aligned}$$

and we conclude as in Proposition 2.1. \square

Proposition 2.4. Assume that \mathbb{C}_Ω and \mathbb{C}_f are strongly elliptic with constants c_Ω and c_f respectively, such that $c_f > c_\Omega > 0$; then there exists a constant $\alpha_4 > 0$, independent of h , such that:

$$\inf_{(u_h, w_h) \in \ker(\mathbb{E}_h)} \sup_{(v_h, y_h) \in \ker(\mathbb{E}_h)} \frac{(\mathbb{C}_\Omega \nabla v_h, \nabla u_h)_\Omega + (\delta \mathbb{C}_f \nabla y_h, \nabla w_h)_{\Omega_f}}{\|(v_h, y_h)\|_{\mathbb{V}} \|(u_h, w_h)\|_{\mathbb{V}}} \geq \alpha_4,$$

where

$$\ker(\mathbb{E}_h) := \left\{ \mathbf{v}_h := (v_h, w_h) \in \mathbb{V}_h : \langle q_h, v_h|_{\Omega_f} - w_h \rangle = 0 \quad \forall q_h \in Q_h \right\}.$$

The proof follows the one of Proposition 2.2.

Error estimate. Proposition 2.1 and 2.2 allow us to apply the theory from Chapter 5 of [10], obtaining the following error estimate:

Theorem 2.1. Consider \mathbb{C}_Ω and \mathbb{C}_f , elastic stress tensors satisfying the hypothesis of Proposition 2.2, the domains Ω and Ω_f with the regularity required in Section 2, and $b \in L^2(\Omega)^d$. Then the following error estimate holds for (u, w, λ) , solution to Problem 3, and (u_h, w_h, λ_h) , solution of Problem 4:

$$\begin{aligned} \|u - u_h\|_V + \|w - w_h\|_W + \|\lambda - \lambda_h\|_Q &\leq \\ C_e \left(\inf_{v_h \in V_h} \|u - v_h\|_V + \inf_{y_h \in W_h} \|w - y_h\|_W + \inf_{q_h \in Q_h} \|\lambda - \lambda_h\|_Q \right), \end{aligned} \quad (28)$$

where $C_e > 0$, and depends on $\alpha_3, \alpha_4, c_\Omega, c_f$ and the norm of the operators \mathcal{K}_Ω and \mathcal{K}_f .

We remark how the constant C_e is affected by the coupling between the two meshes; as intuition suggests, the quality of the solution does not depend only on the ability of V and W to individually describe it, but also on the coupling between them.

Non-matching meshes. One of the basic assumptions made in the continuous case is that, for every element $v \in V$, we have that $v|_{\Omega_f} \in W$; similarly every element $w \in W$ can be extended to an element of V .

With an independent discretization of the two meshes, the inclusion $W_h \subset V_h$ is in general false. In this case, the two requirements for a good approximation of the problem are that the projection $P_W: W \rightarrow W_h$ is H^1 -stable, and that the kernel of \mathbb{E}_h is “rich enough”.

The H^1 stability condition can be easily obtained by inverse inequalities on quasi-uniform meshes. For more general meshes, the stability of the L^2 projection has been investigated, for example, in [17, 15, 7]. The non-matching nature of the discretization does not deteriorate the approximation properties of the underlying spaces, provided that the two discretizations have comparable local mesh sizes.

In particular, the triangle inequality and Bramble-Hilbert lemma imply readily that for any u in V we can write

$$\begin{aligned} \left\| u|_{\Omega_f} - P_W \left((P_V u)|_{\Omega_f} \right) \right\|_{\Omega_f} &\leq \left\| u|_{\Omega_f} - (P_V u)|_{\Omega_f} \right\|_{\Omega_f} + \\ &\quad \left\| (P_V u)|_{\Omega_f} - P_W \left((P_V u)|_{\Omega_f} \right) \right\|_{\Omega_f} \\ &\leq C_V h_V \left| u|_{\Omega_f} \right|_{H^1(\Omega_f)} + C_W h_W \left| (P_V u)|_{\Omega_f} \right|_{H^1(\Omega_f)}, \end{aligned} \quad (29)$$

i.e., even with non-matching meshes, the passage through the two non-matching discretizations still allows one to control in a straight forward way the L^2 norm of the error for any H^1 function on Ω . Provided that the discretizations on Ω and Ω_f have comparable mesh sizes (respectively h_V and h_W in the equation above), then the passage through non-matching meshes keeps the error in the same order.

Moreover, if we integrate exactly on the non-matching grids, it is possible to guarantee that globally constant and linear functions are included in the kernel, ensuring that $\ker(\mathbb{E}_h) \neq \{(0, 0)\}$.

3. Thin fibers

The computational cost of discretizing numerous three-dimensional fibers might render Problem 4 too computationally demanding: a possible simplification is to approximate the fibers with one-dimensional structures. This construction is a non-trivial because the restriction (or trace) of a three-dimensional function to a one-dimensional domain is not well defined in the H^1 Sobolev space, which is the natural space where the elasticity problem is well posed.

Instead of resorting to weighted Sobolev spaces and graded meshes, as done in [19, 18], we define the coupling between the one-dimensional fibers and the three-dimensional elastic matrix through an averaging technique that renders the problem well posed.

To simplify the exposition, we consider a single fiber with constant radius a ; the same results hold for a finite collection of fibers. Given a one-dimensional curve Γ immersed in \mathbb{R}^3 , we call *fiber* its tubular extension of radius $a > 0$:

$$\Omega_f := \{x \in \mathbb{R}^3 : \text{dist}(x, \Gamma) \leq a\},$$

such that $\partial\Omega_f$ is non-intersecting.

Given a point x on Γ , we call $D_a(x)$ the disk of radius a orthogonal to Γ , and we assume that the fibers can be written as the image of a diffeomorphism

$$\Phi: \Omega_a \rightarrow \Omega_f, \quad (30)$$

where Ω_a is a straight cylinder of radius a and of axis Υ aligned with the coordinate x_1 , and Φ satisfies the following hypotheses:

- i) $\Phi(\Omega_a) = \Omega_f$
- ii) $\Phi(\Upsilon) = \Gamma$
- iii) $D_a(\Phi(x)) = \Phi(D_a(x))$, for every $x \in \Upsilon$.

Given two vectors $u, v \in \mathbb{R}^n$, their tensor product is a matrix of size $n \times n$, denoted as $u \otimes v$; defined for each index $i, j \in \mathbb{N}$, $1 \leq i, j \leq n$ as:

$$(u \otimes v)_{i,j} := u_i v_j.$$

Let $W := H^1(\Omega_f)^d$, and $W_\Gamma := H^1(\Gamma)^d$. For $w \in W_\Gamma$, the surface gradient along the curve is defined as:

$$\nabla_\Gamma w := t \otimes t \nabla \varphi_w, \quad (31)$$

where t is the unitary tangent vector to the curve Γ and φ_w is a smooth extension of w in a tubular neighborhood of Γ .

The following result can be used to define the coupling between the three dimensional elastic matrix and the one dimensional fibers:

Theorem 3.1. *Let Ω_f be a fiber of radius a with center line Γ .*

The operator $\mathcal{R}: W \rightarrow W_\Gamma$, defined as

$$\mathcal{R}u(x) := \frac{1}{|D_a(0)|} \int_{D_a(x)} u(y) dD_y, \quad x \in \Gamma \quad (32)$$

is bounded and continuous.

Proof. We start by considering straight cylinders, and smooth functions. Let $u \in C^\infty(\Omega_a)$; the following inequalities hold:

$$\|\mathcal{R}u\|_\Upsilon \leq \frac{1}{\sqrt{\pi}a} \|u\|_{\Omega_a} \quad (33)$$

$$\|\nabla_\Upsilon \mathcal{R}u\|_\Upsilon \leq \frac{1}{\sqrt{\pi}a^2} \|\nabla u\|_{\Omega_a}, \quad (34)$$

where Ω_a is a straight cylinder of axis Υ .

Consider the coordinates (x_1, x_2, x_3) , where x_1 is aligned with the cylinder's axis and x_2, x_3 are normal to the axis. The first inequality can be proven directly, using either Jensen's or Hölder inequality:

$$\begin{aligned} \|\mathcal{R}u\|_\Upsilon^2 &= \frac{1}{(\pi a^2)^2} \int_\Upsilon \left(\int_{D_a(x_1)} u(x_1, x_2, x_3) dx_2 dx_3 \right)^2 dx_1 \\ &\leq \frac{1}{\pi a^2} \int_\Upsilon \int_{D_a(x_1)} u(x_1, x_2, x_3)^2 dx_2 dx_3 dx_1 = \frac{1}{\pi a^2} \|u\|_{\Omega_a}^2 \end{aligned}$$

The second inequality can be proven in a similar fashion, by splitting the integral used to compute $\mathcal{R}u(x)$ on Γ and on the domain $D := \{x_2, x_3 \text{ s.t. } x_2^2 + x_3^2 \leq a^2\}$, which does not depend on x_1 , and observing that $|\nabla_\Gamma \mathcal{R}u(x)|^2 = |\partial_{x_1} \mathcal{R}u(x)|^2$.

From (33) and (34), we conclude with a density argument that

$$u \in H^1(\Omega_a)^d \Rightarrow \mathcal{R}u \in H^1(\Upsilon)^d.$$

The generalization to a generic fiber $\Omega_f = \Phi(\Omega_a)$ follows applying a change of coordinate transformation through Φ . In particular, for any $u \in H^1(\Omega_a)$:

$$\|u \circ \Phi\|_{H^1(\Omega_a)} \leq C_J^{1/2} C_\Phi \|u\|_{H^1(\Omega_f)} \quad (35)$$

$$\|\mathcal{R}u\|_{H^1(\Gamma)} \leq (C_J C_\Phi)^{3/2} \|\mathcal{R}(u \circ \Phi)\|_{H^1(\Upsilon)}, \quad (36)$$

where we defined the following positive constants:

$$C_J := \sup_{z \in \Omega_f} |J\Phi^{-1}(z)| \quad C_\Phi := \sup_{z \in \Omega_f} |\nabla\Phi(z)|.$$

For the first inequality, we begin with the L^2 part of the norm:

$$\|u \circ \Phi\|_{\Omega_a}^2 = \int_{\Omega_a} (u \circ \Phi)^2 d\Omega_a = \int_{\Omega_f} u^2 |J\Phi^{-1}| d\Omega_f \leq C_J \|u\|_{\Omega_f}^2.$$

Similarly, for $\|\nabla(u \circ \Phi)\|_{\Omega_a}^2$:

$$\begin{aligned} \|\nabla(u \circ \Phi)\|_{\Omega_a}^2 &= \int_{\Omega_a} (\nabla(u \circ \Phi)(z))^2 d\Omega_a \\ &= \int_{\Omega_a} (\nabla\Phi(z)^T \nabla u(\Phi(z)))^2 d\Omega_a \leq C_\Phi^2 \int_{\Omega_a} (\nabla u(\Phi(z)))^2 d\Omega_a \\ &= \int_{\Omega_f} (\nabla u(\tilde{z}))^2 |J\Phi^{-1}| d\Omega_f \leq C_J C_\Phi^2 \|u\|_{\Omega_f}^2. \end{aligned}$$

To prove the second inequality we follow a similar procedure, splitting the integral over the centerline of the tubular neighbourhood and the restrictions of Φ to the perpendicular disks. The combined inequalities imply the thesis:

$$\|\mathcal{R}u\|_{H^1(\Gamma)} \leq C \|u\|_{H^1(\Omega_f)}. \quad (37)$$

□

A possible right inverse of the restriction operator is the extension operator \mathcal{E} :

$$\begin{aligned} \mathcal{E}: H^1(\Gamma)^d &\rightarrow H^1(\Omega_f)^d, \\ w &\rightarrow w \circ P_\Gamma, \end{aligned}$$

where P_Γ is the geometric projection from the domain Ω_f to Γ , i.e., for every $y \in \Omega_f$, $P_\Gamma y$ is the element of Γ such that:

$$\text{dist}(y, P_\Gamma y) \leq \text{dist}(y, x) \quad \text{for every } x \in \Gamma.$$

Equation (30) guarantees that P_Γ is well-defined. The operator \mathcal{E} is clearly bounded in L^2 ; to prove that its gradient is bounded it is sufficient to adapt the proof of Theorem 3.2.

The following result allows us to define a function g on Γ , describing the geometry of Ω_f , and reduce our computations to a linear integration.

Theorem 3.2. For a general tubular neighbourhood Ω_f of a curve Γ , for which the curvature κ and the torsion τ are defined a.e., there exists a function g defined on Γ satisfying:

$$\frac{1}{2}(\delta\mathbb{C}_f\nabla\mathcal{E}w, \nabla\mathcal{E}w)_{\Omega_f} = \frac{c_\Gamma}{2}(g\delta\mathbb{C}_f\nabla_\Gamma w, \nabla_\Gamma w)_\Gamma, \quad (38)$$

for every $w \in H^1(\Gamma)^d$, with $c_\Gamma := \pi a^2$.

Proof. Let I be an interval, and let $\omega: I \rightarrow \Gamma$ be the arclength parametrization of Γ . From the hypotheses, it is possible to define an orthonormal basis on Γ : the tangent $t(s)$, the normal $n(s)$, and the binormal $b(s)$, along with the curvature $\kappa(s)$ and the torsion $\tau(s)$ (see, e.g., [38]).

We consider a change of coordinates w.r.t. t , n , and b , which is typically used in physics to study wave propagation, optics and particle trajectories [41, 60, 58], based on the coordinates (r, ϑ, s) , with the orthogonal metric:

$$dx \cdot dx = dr^2 + r^2 d\vartheta^2 + (1 - \kappa r \cos(\vartheta - \hat{\theta}))^2 ds^2,$$

and the explicit formula for the gradient:

$$\nabla \cdot := \frac{d \cdot}{dr} e_1 + \frac{1}{r} \frac{d \cdot}{d\vartheta} e_2 + \frac{1}{1 - \kappa(s)r \cos(\vartheta - \hat{\theta})} \frac{d \cdot}{ds} t. \quad (39)$$

For a detailed description of these formulas, and the exact definition of the angles ϑ and $\hat{\theta}$ see [58, Chapter 3].

Given $w \in H^1(\Gamma)^d$ the extension $\mathcal{E}w$ is constant on each orthogonal disk, i.e., when computing the gradient with Equation (39) the components e_r and e_θ are 0.

Thus:

$$\begin{aligned} (\delta\mathbb{C}_f\nabla\mathcal{E}w, \nabla\mathcal{E}w)_{\Omega_f} &= \int_{\Omega_f} \delta\mathbb{C}_f\nabla\mathcal{E}w\nabla\mathcal{E}w d\Omega \\ &= \int_\Gamma \left(\int_{D_a(s)} \delta\mathbb{C}_f\nabla_\Gamma w(s)\nabla_\Gamma w(s) dr d\theta \right) ds \\ &= \int_\Gamma \left(\int_{D_a(s)} \frac{1}{1 - \kappa(s)r \cos(\theta - \hat{\theta})} \delta\mathbb{C}_f \frac{d}{ds} w(s) \frac{d}{ds} w(s) dr d\theta \right) ds \\ &= \int_\Gamma \delta\mathbb{C}_f\nabla_\Gamma w(s)\nabla_\Gamma w(s) \underbrace{\left(\int_{D_a(s)} \frac{1}{1 - \kappa(s)r \cos(\theta - \hat{\theta})} dr d\theta \right)}_{=: g(s)\pi a^2} ds \\ &= (g\delta\mathbb{C}_f\nabla_\Gamma w, \nabla_\Gamma w)_\Gamma. \end{aligned}$$

Where we defined the function:

$$g(s) := \frac{1}{\pi a^2} \int_{D_a(s)} \frac{1}{1 - \kappa(s)r \cos(\theta - \hat{\theta})} dr d\theta.$$

□

The function g encodes a geometrical stiffness information, which reflects the fact that rods with finite thickness store more energy (i.e., the function g grows) when they are bent with high curvature w.r.t. to their thickness (i.e., when κr is close to one). In the case of a straight cylinder $\kappa(s) = 0$ a.e., and g reduces to the constant one.

The condition $r \leq a < \max_s 1/\kappa(s)$, which is necessary to guarantee that Ω_f is non self-intersecting [20], plays a major role also in defining the geometrical stiffness g on the whole disk. Under these hypotheses it is also possible to prove that there exists a constant $C_g > 0$ such that $g(s) \geq C_g > 0$.

3.1. Problem Formulation

When the fibers are thin compared to the domain size (i.e., $a \ll \text{diam}(\Omega)$), it is reasonable to make the following assumptions:

- i) during the deformation, the radius of the fibers does not change;
- ii) the deformation field inside the fiber is similar to the deformation on the centerline of the fiber itself.

If we consider then a solution u to Problem (3), we expect that

$$\mathcal{E}R u \simeq u|_{\Omega_f}, \quad (40)$$

justifying the replacement of the space $W \subseteq H^1(\Omega_f)^d$ with the much smaller space $\mathcal{E}W_\Gamma \subset W \subseteq H^1(\Omega_f)^d$.

If we restrict functions in W in Problem (4) to the subspace $\mathcal{E}W_\Gamma$, and exploit Theorem 3.2 and the fact that $\mathcal{R}\mathcal{E}w = w$ for any $w \in W_\Gamma$, we obtain the following energy functional for thin fibers

$$\psi_T(u, w, \lambda) = \frac{1}{2}(\mathbb{C}_\Omega \nabla u, \nabla u)_\Omega + c_\Gamma(g\delta\mathbb{C}_f \nabla_\Gamma w, \nabla_\Gamma w)_\Gamma + \langle q, \mathcal{R}u - w \rangle - (b, u)_\Omega,$$

where the non-slip condition on Ω_f has been replaced by an *average* non-slip condition:

$$\langle q, \mathcal{R}u - w \rangle = 0 \quad \forall q \in Q_\Gamma,$$

where $Q_\Gamma := W'_\Gamma$, and here and below the notation $\langle \cdot, \cdot \rangle$ is used to indicate the duality product between $Q'_\Gamma = W_\Gamma$ and $Q_\Gamma := W'_\Gamma$.

We obtain the following formulation for the coupling of thin fibers with a thick elastic matrix:

Problem 5 (1D-3D Weak Formulation). *Given $b \in L^2(\Omega)^d$, find $u \in V, w \in W_\Gamma, \lambda \in Q_\Gamma$ such that:*

$$\begin{aligned} (\mathbb{C}_\Omega \nabla u, \nabla v)_\Omega + \langle \lambda, \mathcal{R}v \rangle &= (b, v)_\Omega & \forall v \in V, \\ c_\Gamma(g\delta\mathbb{C}_f \nabla_\Gamma w, \nabla_\Gamma y)_\Gamma - \langle \lambda, y \rangle &= 0 & \forall y \in W_\Gamma, \\ \langle q, \mathcal{R}u - w \rangle &= 0 & \forall q \in Q_\Gamma. \end{aligned}$$

Similarly to what was done in the full order problem, we define the space $\mathbb{V} := V \times W_\Gamma$, its norm $\|(\cdot, \cdot)\|_{\mathbb{V}} := \|\cdot\|_V + \|\cdot\|_{W_\Gamma}$, and the operators:

$$\begin{aligned} \mathbb{F}_T &:= (\mathbb{C}_\Omega \nabla u, \nabla v)_\Omega + c_\Gamma(g\delta\mathbb{C}_f \nabla_\Gamma w, \nabla_\Gamma w)_\Gamma, \\ \mathbb{E}_T &:= \langle q, \mathcal{R}u - w \rangle. \end{aligned}$$

3.2. Well-posedness, existence and uniqueness

Proposition 3.1. *There exists a constant $\alpha_5 > 0$ such that:*

$$\inf_{q \in Q_\Gamma} \sup_{(v,w) \in \mathbb{V}} \frac{\langle q, \mathcal{R}v - w \rangle}{\|(v,w)\|_{\mathbb{V}} \|q\|_{Q_\Gamma}} \geq \alpha_5,$$

where:

$$\ker \mathbb{E}_T := \{ \mathbf{v} := (v,w) \in \mathbb{V} : \langle q, \mathcal{R}v - w \rangle = 0 \ \forall q \in Q_\Gamma \}.$$

Moreover $\alpha_5 = 1$.

Proof. The non slip condition is given by the duality pairing between $Q_\Gamma = W'_\Gamma$ and W ; by definition of the norm in the dual space Q_Γ :

$$\|q\|_{Q_\Gamma} = \sup_{w \in W_\Gamma} \frac{\langle q, w \rangle}{\|w\|_W} \leq \sup_{v \in V, w \in W_\Gamma} \frac{\langle q, \mathcal{R}v - w \rangle}{(\|w\|_W^2 + \|v\|_V^2)^{\frac{1}{2}}},$$

where the last inequality can be proven fixing $v = 0$.

The final statement is found dividing by $\|q\|_{Q_\Gamma}$ and taking the $\inf_{q \in Q_\Gamma}$. \square

Proposition 3.2. *Assume \mathbb{C}_Ω and \mathbb{C}_f are strongly elliptic, with constants c_Ω and c_f respectively such that $c_\Omega > c_f > 0$; there exists a constant $\alpha_6 > 0$ such that:*

$$\inf_{(u,w) \in \ker \mathbb{E}_T} \sup_{(v,y) \in \ker \mathbb{E}_T} \frac{(\mathbb{C}_\Omega \nabla v, \nabla u)_\Omega + c_\Gamma (g\delta \mathbb{C}_f \nabla_\Gamma y, \nabla_\Gamma w)_\Gamma}{\|(v,y)\|_{\mathbb{V}} \|(u,w)\|_{\mathbb{V}}} \geq \alpha_6.$$

Proof. For every $(u,w) \in \ker \mathbb{E}_T$:

$$\begin{aligned} & \sup_{(v,y) \in \ker(\mathbb{E}_T)} \frac{(\mathbb{C}_\Omega \nabla u, \nabla v)_\Omega + c_\Gamma (g\delta \mathbb{C}_f \nabla_\Gamma w, \nabla_\Gamma y)_\Gamma}{\|(v,y)\|_{\mathbb{V}}} \\ & \geq \frac{c_\Omega (\nabla u, \nabla u)_\Omega + c_\Gamma C_g (c_f - c_\Omega) (\nabla_\Gamma w, \nabla_\Gamma w)_\Gamma}{\|(u,w)\|_{\mathbb{V}}} \\ & \geq \frac{c_p c_\Gamma c_b \min(c_\Omega, C_g (c_f - c_\Omega))}{2} \frac{(u,u)_{H^1(\Omega)} + (w,w)_{H^1(\Gamma)}}{\|(u,w)\|_{\mathbb{V}}} \\ & \geq \alpha_6 \|(u,w)\|_{\mathbb{V}}, \end{aligned}$$

with $\alpha_6 := \frac{c_p c_\Gamma c_b \min(c_\Omega, C_g (c_f - c_\Omega))}{2}$.

The result is obtained dividing and considering the $\inf_{(u,w) \in \ker \mathbb{E}_T}$. \square

Using the saddle point theory we conclude that Problem 5 is well-posed, and has a unique solution.

3.3. Finite element discretization

The discretization of Problem 5 for thin fibers follows the steps of Section 2.3, on the domains Ω and Γ (the fiber's one-dimensional core). Consider two independent discretizations for these domains; the family $\mathcal{T}_h(\Omega)$ of regular meshes in Ω , and a family $\mathcal{T}_h(\Gamma)$ of regular meshes in Γ . We assume no geometrical error is committed when meshing and consider two independent finite element discretizations $V_h \subset V$, $W_h \subset W_\Gamma$, and let $Q_h = W_h$.

Problem 6 (1D-3D Discretized Weak Formulation). *Given $b \in L^2(\Omega)^d$, find $u_h \in V_h, w_h \in W_h, \lambda_h \in Q_h$ such that:*

$$(\mathbb{C}_\Omega \nabla u_h, \nabla v_h)_\Omega + \langle \lambda_h, \mathcal{R}v_h \rangle = (b, v_h)_\Omega \quad \forall v_h \in V_h, \quad (41)$$

$$c_\Gamma (g\delta \mathbb{C}_f \nabla_\Gamma w_h, \nabla_\Gamma y_h)_\Gamma - \langle \lambda_h, y_h \rangle = 0 \quad \forall y_h \in W_h, \quad (42)$$

$$\langle q_h, \mathcal{R}u_h - w_h \rangle = 0 \quad \forall q_h \in Q_h. \quad (43)$$

Again, existence, well posedness and convergence are guaranteed if the classical inf-sup conditions are satisfied:

Proposition 3.3. *Assume the L^2 projection $P_{W_\Gamma}: W_\Gamma \rightarrow W_h$ is continuous and H^1 -stable, as in Proposition 2.3; then there exists a constant $\alpha_7 > 0$, independent of h , such that:*

$$\inf_{q_h \in W_h} \sup_{(v_h, w_h) \in \mathbb{V}_h} \frac{(q_h, \mathcal{R}v_h - w_h)_\Gamma}{\|(v_h, w_h)\|_{\mathbb{V}} \|q_h\|_\Gamma} \geq \alpha_7.$$

Proposition 3.4. *Assume \mathbb{C}_Ω and \mathbb{C}_f are strongly elliptic, with constants c_Ω and c_f respectively such that $c_f > c_\Omega > 0$; then there exists a constant $\alpha_8 > 0$, independent of h , such that:*

$$\inf_{(u_h, w_h) \in \ker \mathbb{E}_{T,h}} \sup_{(v_h, y_h) \in \ker \mathbb{E}_{T,h}} \frac{(\mathbb{C}_\Omega \nabla v_h, \nabla u_h)_\Omega + c_\Gamma (g\delta \mathbb{C}_f \nabla_\Gamma y_h, \nabla_\Gamma w_h)_\Gamma}{\|(v_h, y_h)\|_{\mathbb{V}} \|(u_h, w_h)\|_{\mathbb{V}}} \geq \alpha_8,$$

where:

$$\ker \mathbb{E}_{T,h} := \{\mathbf{v}_h := (v_h, w_h) \in \mathbb{V}_h : \langle q_h, \mathcal{R}v_h - w_h \rangle = 0 \quad \forall q_h \in Q_h\}.$$

The proofs of these propositions are variations on the proof Propositions 2.3 and 2.4. It is possible to prove an estimate analogous to the one of Theorem 2.1:

Theorem 3.3. *Consider \mathbb{C}_Ω and \mathbb{C}_f , elastic stress tensors satisfying the hypothesis of Proposition 3.2, the domains Ω and Ω_f with the regularity required in this section, and $b \in L^2(\Omega)^d$. Then the following error estimate holds for (u, w, λ) , solution to Problem 5, and (u_h, w_h, λ_h) , solution of Problem 6:*

$$\|u - u_h\|_V + \|w - w_h\|_{W_\Gamma} + \|\lambda - \lambda_h\|_{Q_\Gamma} \leq C_e \left(\inf_{v_h \in V_h} \|u - v_h\|_V + \inf_{y_h \in W_h} \|w - y_h\|_{W_\Gamma} + \inf_{q_h \in Q_h} \|\lambda - \lambda_h\|_{Q_\Gamma} \right), \quad (44)$$

where $C_e > 0$, and depends on $\alpha_5, \alpha_6, c_\Omega, c_f$ and the norms of the operators $\mathcal{K}_\Omega: V \rightarrow V'$ defined as $\langle \mathcal{K}_\Omega u, \cdot \rangle := (\mathbb{C}_\Omega \nabla u, \nabla \cdot)_\Omega$, and $\mathcal{K}_f: W_\Gamma \rightarrow Q_\Gamma$ defined as $\langle \mathcal{K}_f w, \cdot \rangle := (\delta \mathbb{C}_f \nabla w, \nabla \cdot)_{\Omega_f}$.

4. Numerical validation

The analytical solution of Problems 3 and 5, even for simple configurations, is non-trivial: we chose some FRMs structures which are studied in literature, and used the known approximated solutions as a comparison for our model.

Using the deal.II library [4, 3, 6, 44, 59], and the deal.II step-60 tutorial [40] we developed a model for thin fibers proposed in Section 3, and compared it with the Rule of Mixtures and the Halpin-Tsai configurations in some pull and push tests.

Numerical Setting. To solve Problem 6 on a collection of fibers we define:

- i) $V_h = \text{span}\{v_i\}_{i=1}^N \subset H^1(\Omega)$, finite element space of dimension $N \in \mathbb{N}$ defined on Ω , the elastic matrix;
- ii) $W_h = \text{span}\{w_a\}_{a=1}^M \subset H^1(\Gamma)$ the finite element discretization of dimension $M \in \mathbb{N}$ defined on the collection of $n_f \in \mathbb{N}$ fibers $\Gamma := \bigcup_{k=1}^{n_f} \Gamma_k \subset \Omega$;
- iii) Q_h : the space of the Lagrange multiplier, discretized as W_h .

We use i, j as indices for the space V_h and a, b as indices for the space W_h , and assume all hypotheses on spaces and meshes of Section 3.3 are satisfied. For each fiber Γ_k we define its tubular neighborhood $\Omega_{a,k}$, and define

$$\Omega_f := \bigcup_{k=1}^{n_f} \Omega_{a,k}.$$

In our implementation, we compute integrals over Ω_f by quadrature formulas, computing the integration over the orthogonal disks $D_a(x)$ to Γ using the mid point rule.

The restriction of the operators of Problem 6 to the discrete finite element spaces produce the following sparse matrices:

$$\begin{aligned} A: V_h &\rightarrow V'_h & A_{ij} &:= (\mathbb{C}_\Omega \nabla v_i, \nabla v_j)_\Omega, \\ K: W_h &\rightarrow W'_h & K_{ab} &:= c_\Gamma (g \delta \mathbb{C}_f \nabla_\Gamma w_a, \nabla_\Gamma w_b)_\Gamma, \\ B: V_h &\rightarrow Q'_h & B_{ia} &:= (v_i|_\Gamma, w_a)_\Gamma, \\ L: W_h &\rightarrow Q'_h & L_{ab} &:= (w_a, w_b)_\Gamma. \end{aligned} \tag{45}$$

Here B is the coupling matrix from V_h to W_h , M the mass-matrix of W_h . The discretization of Problem 6 becomes: find $(u, w, \lambda_h) \in V_h \times W_h \times Q_h$ such that

$$\begin{pmatrix} A & 0 & B^T \\ 0 & K & -L^T \\ B & -L & 0 \end{pmatrix} \begin{pmatrix} u \\ w \\ \lambda \end{pmatrix} = \begin{pmatrix} g \\ 0 \\ 0 \end{pmatrix}, \tag{46}$$

where $g_i := (b, v_i)_\Omega$. We reduce the system through the solution of the following linear problems:

$$\begin{aligned} Kw &= L^T \lambda = L \lambda \Rightarrow \lambda = L^{-1} Kw, \\ Bu &= Lw \Rightarrow w = L^{-1} Bu, \end{aligned}$$

obtaining:

$$(A + B^T L^{-1} K L^{-1} B)u = (A + P_\Gamma^T K P_\Gamma)u = g, \tag{47}$$

where $P_\Gamma := L^{-1} B$. Boundary conditions are imposed weakly, using Nitsche method as done in [56].

4.1. Model description

For our simulations we use linear finite elements and uniformly refined hexaedral meshes. The elastic matrix is the unitary cube $\Omega := [0, 1]^3$, where for boundary conditions we refer to Figure 3b. The used elastic tensors are described in Equations 20-22; for the model description we use the following parameters:

- r_Ω, r_Γ : global refinements of the meshes describing Ω and Γ respectively.
- $\lambda_\Omega, \mu_\Omega, \lambda_f, \mu_f$: Lamé parameters for the elastic matrix and the fibers respectively.
- β : fiber volume ratio or representative volume element (RVE), i.e., $\beta = |\Omega_f|/|\Omega|$.
- a : the radius of the fibers.

4.2. Homogeneous fibers

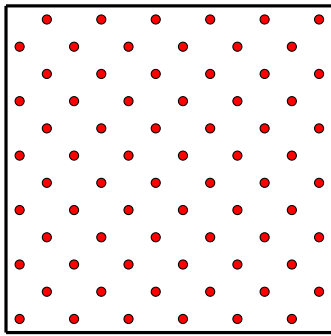
We consider a unidirectional composite, where fibers are uniform in properties and diameter, continuous, and parallel throughout the composite Ω (see Figure 3a). We compare the results obtained with our model with the ones obtained using the Rule of Mixtures [25, 2] to approximate the stress-strain equation:

$$S[u] = \frac{1}{2}(\mathbb{C}_\Omega Eu, Eu)_\Omega + \beta \frac{1}{2}(\delta \mathbb{C}_f Eu, Eu)_\Omega. \quad (48)$$

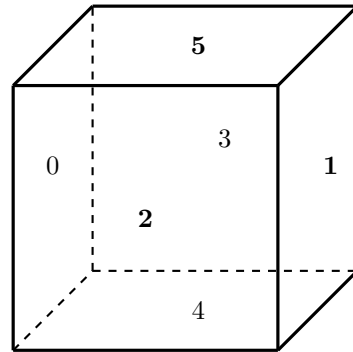
This approximation agrees with experimental tests especially for tensile loads, and when the fiber ratio β is small.

Multiple tests were run, keeping β constant, while increasing the fiber density and reducing the fiber diameter; we expect this process to render the coupled model solution increasingly close to the homogenized one.

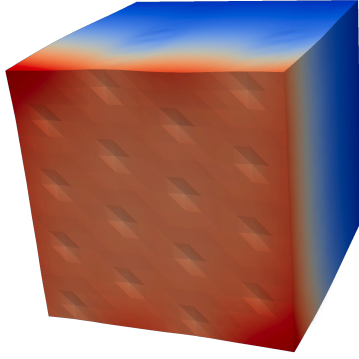
Comparing solutions. Figures 4a and 4b illustrate the influence of Ω 's refinement on the final result, when using few fibers on a pull test. Stiff fibers oppose being stretched, deforming the elastic matrix Ω through the non-slip condition: near each fiber, the deformation of Ω should be symmetrical, resembling a cone. This effect is better described in Figure 4b, where the higher value of r_Ω results in greater geometrical flexibility of the elastic matrix, allowing a better description of the effect of each fiber. Lower values of r_Ω result in a non symmetrical solution, as in Figure 4a. The lower geometrical flexibility results in an “averaged” solution which, in the case of few fibers, is closer to the homogenized model.



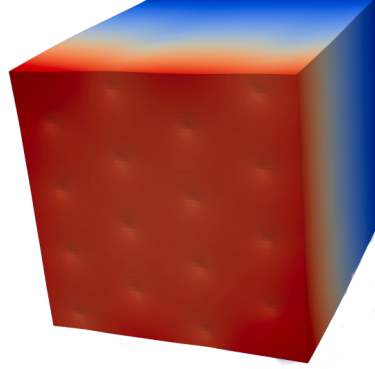
(3a) Section with homogeneous fibers.



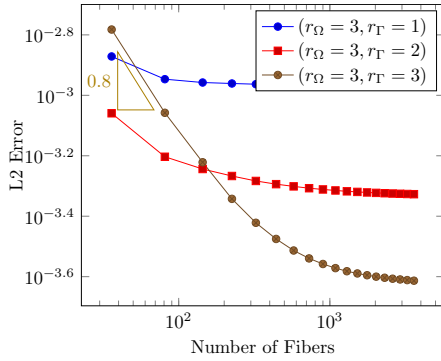
(3b) Ω 's faces numbering



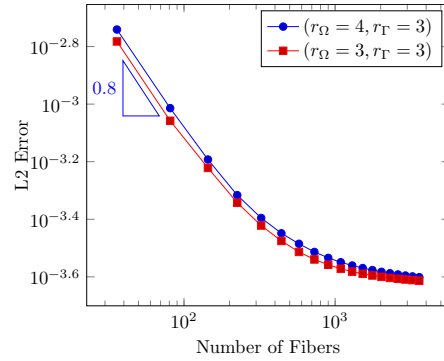
(4a) Pull test example, with $r_\Omega = 4$



(4b) Pull test example, with $r_\Omega = 6$



(5a) Pull Test, $\lambda = \lambda_F = 0.4$, $\mu = 1$, $\mu_F = 1000$, $\beta = 0.1$.



(5b) Pull Test, $\lambda = \lambda_F = 0.4$, $\mu = 1$, $\mu_F = 1000$, $r_\Omega = 3$, $r_\Gamma = 3$.

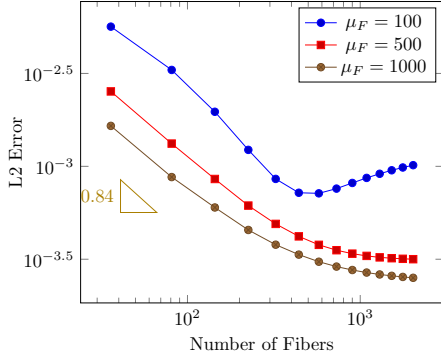
The slopes in the plots have been computed by taking the ratio of the error in two subsequent simulation, i.e.,

$$\frac{\ln(\mathbf{e}_2/\mathbf{e}_1)}{\ln(n_{f,2}/n_{f,1})},$$

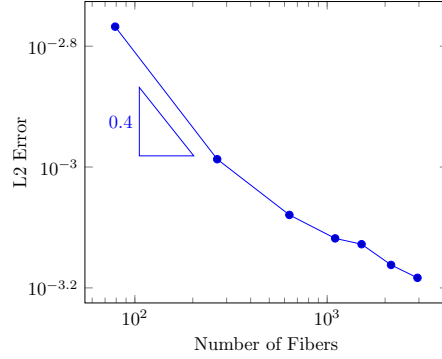
where $\mathbf{e}_1, \mathbf{e}_2$ be the L^2 errors and $n_{f,1}, n_{f,2}$ be the number of fibers for two subsequent simulations.

Pull test along fibers. Dirichlet homogeneous conditions is applied to face 0, Neumann homogeneous conditions is applied to faces 2,3,4,5. In the Push Test, the Neumann condition 0.05 is applied to face 1. For the Pull Test, the value -0.05 is applied to the same face. Boundary conditions are applied only to $\partial\Omega$; the fibers interact through the coupling with the elastic matrix. We report here only data from pull tests, as push tests gave comparable results.

The use of the projection matrix $P_\Gamma: V_h \rightarrow W_h$, and the error estimate for the fully



(6a) Pull Test with varying μ_F , $\lambda = \lambda_F = 0.4$, $\mu = 1$, $\beta = 0.1$, $r_\Omega = 3$, $r_\Gamma = 3$



(6b) Random Pull Test with one dimensional approximation; $r_\Omega = 4$, $r_\Gamma = 2$.

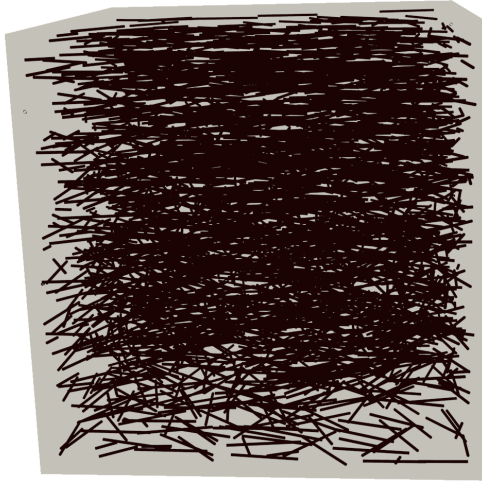


Figure 7: Random Fibers Disposition

three-dimensional case (Inequality 28), both suggest that the solution quality on the elastic matrix depends on both V_h and W_h . This is apparent in Figure 5a, where for $r_\Gamma = 1$ the mesh of Γ is unable to describe the stretch of the material, resulting in the error remaining approximately constant after a certain fiber density is reached. A similar behaviour emerges in the case $r_\Gamma = 2$. Figure 5b shows that refining only the elastic matrix does not improve the solution quality: as the number of fibers increases, the error converges to approximately the same value, which is limited by r_Γ .

Figure 6a shows an error comparison as the value of μ_F varies: as expected our model is better suited for stiff fibers.

Fiber length	0.6	0.4	0.3	0.25	0.225	0.2	0.18
Fiber radius	0.03	0.02	0.015	0.0125	0.01125	0.01	0.009
Number of Fibers	79	268	637	1100	1509	2149	2947

Table 1: Fiber Parameters

4.3. Random fibers

We consider a pull test on a random chopped fiber reinforced composite: we distribute small fibers at a random points of Ω , with a random direction parallel to the $\langle x, y \rangle$ plane; the fibers share the same size and properties. If a fiber surpasses the edge of Ω , it is cut.

For more details on the algorithm used to distribute the fibers see the Random Sequential Adsorption algorithm [51]; our implementation generates only the plane angle, and does not implement an intersection-avoidance mechanism.

As a comparison model, we estimate the material parameters using the empirical Halpin-Tsai [24]; which we report here for longitudinal moduli, as described in [2]. The fibers have length l , diameter d , the fiber and the matrix Young moduli are E_f and E_m respectively, β is the volume fraction occupied by the fibers. We define two empirical constants:

$$\eta_L = \frac{(E_f/E_m) - 1}{(E_f/E_m) + (2l/d)}, \quad \eta_T = \frac{(E_f/E_m) - 1}{(E_f/E_m) + 2}.$$

This allows to compute the longitudinal and transverse moduli for aligned short fibers:

$$E_L = \frac{1 + (2l/d)\eta_L\beta}{1 - \eta_L\beta}, \quad E_T = \frac{1 + 2\eta_T\beta}{1 - \eta_T\beta}.$$

If fibers are randomly oriented in a plane the following equations can be used to predict the elastic modulus:

$$E_C = \frac{3}{8}E_L + \frac{5}{8}E_T, \quad \mu_C = \frac{1}{8}E_L + \frac{1}{4}E_T.$$

Since a random fiber composite is considered isotropic in its plane, the Poisson's ratio can be calculated as:

$$\nu_R = \frac{E_C}{2\mu_C} - 1. \quad (49)$$

According to this approximation, the properties of this composite do not depend directly on the fiber length or radius, but on the aspect ratio l/d . Our test setting runs on the unitary cube, with a fiber ratio $\beta = 0.135$ and a fiber aspect ratio of $\frac{l}{2r} \approx 10$, where l is the fiber's length and r is the fiber's radius; the values used are described in Table 1.

We could not find an exact estimate of the error convergence, but we expect the solution to improve as the number of fibers increases because:

- the fiber radius a reduces, improving of the average non-slip condition,
- more fibers result in a more homogeneous material on the planes parallel to the $\langle x, y \rangle$ plane.

Following [51], we consider a short fiber E-glass/urethane composite: the fiber and matrix Young's modulus are, respectively, $E_f = 70GPa$ and $E_m = 3GPa$, while the Poisson ratios are $\nu_f = 0.2$ and $\nu_m = 0.38$. These values were converted to the Lamé parameters using the classic formulas for hyper elastic materials.

The predicted parameters for the composite are: $E_C = 2.20GPa$ and $\nu_C = 0.38GPa$; these are slightly different from [51] because, in the Halpin-Tsai equations, l/d was used instead of $2l/d$. The boundary conditions used for the pull tests are the same of Paragraph 4.2.

We limit the global refinements of Γ , in order to obtain cells of approximately the same size on both Ω and the fibers. The results are shown in Figure 6b: as the number of fiber increases the error reduces, but because the random fiber model is more complex than the homogeneous one, the final error achieved is higher than the one reached in the previous test.

5. Conclusions

Starting from a linearly elastic description of bi-phasic materials, we derive a new formulation for fiber reinforced materials where independent meshes are used to discretize the fibers and the elastic matrix, and the coupling between the two phases is obtained via a distributed Lagrange multiplier.

We prove existence and uniqueness of a solution for the final saddle point problem, and we analyze a simplified model where fibers are discretised as one-dimensional.

The model is validated against the Rule of Mixtures and the Halpin-Tsai equations, where we test our discretisation with uniform and random distributions of fibers. The true benefit of our model, however, lies in the possibility to tackle complex and intricate fiber structures independently from the background elastic matrix discretization, opening the way to the efficient simulation of complex multi-phase materials.

From the numerical analysis point of view, there are some issues that deserve further development, such as finding better preconditioners for the final system, and exploring different solutions for the one dimensional coupling operator.

The formulation of our method makes it particularly suited for extensions to more complex situations, e.g., three-phasic materials, or materials where perfect-bond is replaced by other, more realistic conditions.

Acknowledgements

The authors would like to thank Prof. Lucia Gastaldi, for the fruitful conversations and suggestions that greatly improved this manuscript, and to thank Dr. Giovanni Noselli, and Dr. Maicol Caponi for their priceless suggestions and insights in their fields of expertise.

Bibliography

- [1] D. F. Adams and D. R. Doner. Transverse normal loading of a unidirectional composite. *Journal of composite Materials*, 1(2):152–164, 1967.
- [2] B. D. Agarwal, L. J. Broutman, and K. Chandrashekhara. *Analysis and performance of fiber composites*. John Wiley & Sons, 2017.

- [3] G. Alzetta, D. Arndt, W. Bangerth, V. Boddu, B. Brands, D. Davydov, R. Gassmoeller, T. Heister, L. Heltai, K. Kormann, M. Kronbichler, M. Maier, J.-P. Pelteret, B. Turcksin, and D. Wells. The deal.II library, version 9.0. *Journal of Numerical Mathematics*, 26(4):173–183, 2018.
- [4] D. Arndt, W. Bangerth, D. Davydov, T. Heister, L. Heltai, M. Kronbichler, M. Maier, J.-P. Pelteret, B. Turcksin, and D. Wells. The deal.II finite element library: Design, features, and insights. *Computers and Mathematics with Applications*, 2020.
- [5] F. Auricchio, D. Boffi, L. Gastaldi, A. Lefieux, and A. Reali. On a fictitious domain method with distributed lagrange multiplier for interface problems. *Applied Numerical Mathematics*, 95:36–50, 2015.
- [6] W. Bangerth, R. Hartmann, and G. Kanschat. deal.II – a general purpose object oriented finite element library. *ACM Trans. Math. Softw.*, 33(4):24/1–24/27, 2007.
- [7] R. E. Bank and H. Yserentant. On the H^1 -stability of the L_2 -projection onto finite element spaces. *Numerische Mathematik*, 126(2):361–381, May 2013.
- [8] R. Barrage, S. Potapenko, and M. A. Polak. Modelling transversely isotropic fiber-reinforced composites with unidirectional fibers and microstructure. *Mathematics and Mechanics of Solids*, page 1081286519838603, 2019.
- [9] T. Behzad and M. Sain. Finite element modeling of polymer curing in natural fiber reinforced composites. *Composites Science and Technology*, 67(7-8):1666–1673, 2007.
- [10] D. Boffi, F. Brezzi, M. Fortin, et al. *Mixed finite element methods and applications*, volume 44. Springer, 2013.
- [11] D. Boffi and L. Gastaldi. A finite element approach for the immersed boundary method. *Computers & structures*, 81(8-11):491–501, 2003.
- [12] D. Boffi and L. Gastaldi. A fictitious domain approach with lagrange multiplier for fluid-structure interactions. *Numerische Mathematik*, 135(3):711–732, 2017.
- [13] D. Boffi, L. Gastaldi, L. Heltai, and C. S. Peskin. On the hyper-elastic formulation of the immersed boundary method. *Computer Methods in Applied Mechanics and Engineering*, 197(25-28):2210–2231, 2008.
- [14] D. Boffi, L. Gastaldi, and M. Ruggeri. Mixed formulation for interface problems with distributed lagrange multiplier. *Computers & Mathematics with Applications*, 68(12):2151–2166, 2014.
- [15] J. H. Bramble, J. E. Pasciak, and O. Steinbach. On the stability of the L_2 projection in H^1 . *Math. Comp*, 71(237):147–156, 2002.
- [16] W. D. Callister, D. G. Rethwisch, et al. *Materials science and engineering: an introduction*, volume 7. John Wiley & Sons New York, 2007.
- [17] M. Crouzeix and V. Thomée. Resolvent estimates in L_p for discrete laplacians on irregular meshes and maximum-norm stability of parabolic finite difference schemes. *Computational Methods in Applied Mathematics*, 1(1):3–17, 2001.
- [18] C. D’Angelo. Finite element approximation of elliptic problems with dirac measure terms in weighted spaces: applications to one-and three-dimensional coupled problems. *SIAM Journal on Numerical Analysis*, 50(1):194–215, 2012.
- [19] C. D’Angelo and A. Quarteroni. On the coupling of 1d and 3d diffusion-reaction equations: application to tissue perfusion problems. *Mathematical Models and Methods in Applied Sciences*, 18(08):1481–1504, 2008.
- [20] J. J. Duistermaat and J. A. Kolk. *Multidimensional real analysis I: differentiation*, volume 86. Cambridge University Press, 2004.
- [21] K. S. Eloh, A. Jacques, and S. Berbenni. Development of a new consistent discrete green operator for fft-based methods to solve heterogeneous problems with eigenstrains. *International Journal of Plasticity*, 116:1–23, 2019.
- [22] M. Goudarzi and A. Simone. Discrete inclusion models for reinforced composites: Comparative performance analysis and modeling challenges. *Computer Methods in Applied Mechanics and Engineering*, 355:535–557, 2019.
- [23] M. E. Gurtin. *An Introduction to Continuum Mechanics*. Mathematics in Science and Engineering 158. Academic Press, 1981.
- [24] J. C. Halpin and J. Kardos. The halpin-tsai equations: a review. *Polymer engineering and science*, 16(5):344–352, 1976.
- [25] Z. Hashin. On elastic behaviour of fibre reinforced materials of arbitrary transverse phase geometry. *Journal of the Mechanics and Physics of Solids*, 13(3):119–134, 1965.
- [26] Z. Hashin. *Theory of fiber reinforced materials*. NASA, Washington, United States, 1972.
- [27] Z. Hashin. Analysis of composite materials—a survey. *Journal of Applied Mechanics*, 50(3):481–505, 1983.

- [28] L. Heltai. On the stability of the finite element immersed boundary method. *Computers & Structures*, 86(7-8):598–617, 2008.
- [29] L. Heltai and A. Caiazzo. Multiscale modeling of vascularized tissues via non-matching immersed methods. *International Journal for Numerical Methods in Biomedical Engineering*, 35(12):e3264, 2019.
- [30] L. Heltai and F. Costanzo. Variational implementation of immersed finite element methods. *Computer Methods in Applied Mechanics and Engineering*, 229-232, 2012.
- [31] L. Heltai and N. Rotundo. Error estimates in weighted sobolev norms for finite element immersed interface methods. *Computers and Mathematics with Applications*, 2019. In press.
- [32] G. A. Holzapfel et al. Biomechanics of soft tissue. *The handbook of materials behavior models*, 3:1049–1063, 2001.
- [33] G. A. Holzapfel and T. C. Gasser. A viscoelastic model for fiber-reinforced composites at finite strains: Continuum basis, computational aspects and applications. *Computer methods in applied mechanics and engineering*, 190(34):4379–4403, 2001.
- [34] G. A. Holzapfel, T. C. Gasser, and R. W. Ogden. A new constitutive framework for arterial wall mechanics and a comparative study of material models. *Journal of elasticity and the physical science of solids*, 61(1-3):1–48, 2000.
- [35] P. A. Huijing. Muscle as a collagen fiber reinforced composite: a review of force transmission in muscle and whole limb. *Journal of biomechanics*, 32(4):329–345, 1999.
- [36] K. Iizuka, M. Ueda, T. Takahashi, A. Yoshimura, and M. Nakayama. Development of a three-dimensional finite element model for a unidirectional carbon fiber reinforced plastic based on x-ray computed tomography images and the numerical simulation on compression. *Advanced Composite Materials*, 28(1):73–85, 2019.
- [37] T. Konopczyński, D. Rathore, J. Rathore, T. Kröger, L. Zheng, C. S. Garbe, S. Carmignato, and J. Hesser. Fully convolutional deep network architectures for automatic short glass fiber semantic segmentation from ct scans. *arXiv preprint arXiv:1901.01211*, 2019.
- [38] E. Kreyszig. *Differential geometry*. University of Toronto Press, 1963.
- [39] S. K. Kyriacou, J. D. Humphrey, and C. Schwab. Finite element analysis of nonlinear orthotropic hyperelastic membranes. *Computational Mechanics*, 18(4):269–278, Jul 1996.
- [40] G. A. L. Heltai. The deal.ii tutorial step-60: non-matching grid constraints through distributed lagrange multipliers. 2018.
- [41] S.-Y. Lee. *Accelerator physics*. World scientific publishing, 2018.
- [42] Z. Lu, Z. Yuan, and Q. Liu. 3d numerical simulation for the elastic properties of random fiber composites with a wide range of fiber aspect ratios. *Computational Materials Science*, 90:123–129, 2014.
- [43] V. Lucas, J.-C. Golinval, S. Paquay, V.-D. Nguyen, L. Noels, and L. Wu. A stochastic computational multiscale approach; application to mems resonators. *Computer Methods in Applied Mechanics and Engineering*, 294:141–167, 2015.
- [44] M. Maier, M. Bardelloni, and L. Heltai. `LinearOperator` – a generic, high-level expression syntax for linear algebra. *Computers and Mathematics with Applications*, 72(1):1–24, 2016.
- [45] P. K. Mallick. *Fiber-reinforced composites: materials, manufacturing, and design*. CRC press, 2007.
- [46] J. E. Marsden and T. J. Hughes. *Mathematical foundations of elasticity*. Courier Corporation, 1994.
- [47] P. K. Mehta. *Concrete. Structure, properties and materials*. McGraw-Hill, 1986.
- [48] H. Moulinec and P. Suquet. A numerical method for computing the overall response of nonlinear composites with complex microstructure. *Computer methods in applied mechanics and engineering*, 157(1-2):69–94, 1998.
- [49] H. Moulinec and P. Suquet. Comparison of fft-based methods for computing the response of composites with highly contrasted mechanical properties. *Physica B: Condensed Matter*, 338(1-4):58–60, 2003.
- [50] T. Nakamura and S. Suresh. Effects of thermal residual stresses and fiber packing on deformation of metal-matrix composites. *Acta metallurgica et materialia*, 41(6):1665–1681, 1993.
- [51] Y. Pan, L. Iorga, and A. A. Pelegri. Analysis of 3d random chopped fiber reinforced composites using fem and random sequential adsorption. *Computational Materials Science*, 43(3):450–461, 2008.
- [52] C. S. Peskin. The immersed boundary method. *Acta Numerica*, 11(1):479–517, jan 2002.
- [53] K. L. Pickering, M. A. Efendy, and T. M. Le. A review of recent developments in natural fibre composites and their mechanical performance. *Composites Part A: Applied Science and Manufacturing*,

- 83:98–112, 2016.
- [54] A. C. Pipkin. Integration of an equation in membrane theory. *Zeitschrift für angewandte Mathematik und Physik ZAMP*, 19(5):818–819, Sep 1968.
 - [55] F. K. F. Radtke, A. Simone, and L. J. Sluys. A computational model for failure analysis of fibre reinforced concrete with discrete treatment of fibres. *Engineering Fracture Mechanics*, 77(4):597–620, 2010.
 - [56] N. Rotundo, T.-Y. Kim, W. Jiang, L. Heltai, and E. Fried. Error analysis of a b-spline based finite-element method for modeling wind-driven ocean circulation. *Journal of Scientific Computing*, 69(1):430–459, 2016.
 - [57] S. Roy, L. Heltai, and F. Costanzo. Benchmarking the immersed finite element method for fluid-structure interaction problems. *Computers and Mathematics with Applications*, 69:1167–1188, 2015.
 - [58] E. Ryder. Nonlinear guided waves in fibre optics. 1993.
 - [59] A. Sartori, N. Giuliani, M. Bardelloni, and L. Heltai. deal2lkit: A toolkit library for high performance programming in deal.II. *SoftwareX*, 7:318–327, 2018.
 - [60] C. Tang. An orthogonal coordinate system for curved pipes (correspondence). *IEEE Transactions on Microwave Theory and Techniques*, 18(1):69–69, 1970.
 - [61] A. Zaoui. Continuum micromechanics: survey. *Journal of Engineering Mechanics*, 128(8):808–816, 2002.